

THERMAL CONVECTION IN A POROUS MEDIUM COMPOSED OF ALTERNATING THICK AND THIN LAYERS

ROBERT MCKIBBIN

Department of Theoretical and Applied Mechanics, University of Auckland, New Zealand

and

PEDER A. TYVAND

Department of Mechanics, University of Oslo, Norway

(Received 4 March 1982 and in final form 23 September 1982)

Abstract—This paper is a continuation of a recent work by the present authors [*J. Fluid Mech.* **118**, 315–339 (1982)]. The previous paper concentrated on buoyancy-driven convection in a porous medium composed of alternating material layers of equal thicknesses. The present work is a study of the limit case where every alternate layer is very thin and has very small permeability. The onset of convection in such a system and the heat flux at slightly supercritical Rayleigh numbers is studied. As in the earlier work, an investigation of the convergence to homogeneous anisotropy is made. Furthermore, emphasis is placed on applications in insulation techniques and convection in snow layers.

NOMENCLATURE

c ,	specific heat of saturating fluid;
d, d_i ,	layer thicknesses;
g ,	gravitational acceleration;
k, k_i, k_v, k_H ,	thermal conductivities of saturated media;
K, K_i, K_v, K_H ,	permeabilities;
l, L, L_c ,	cell or system widths;
N ,	number of layers in system;
Nu ,	Nusselt number;
p, p_a, p_c, p' ,	pressures;
Q, Q_c ,	average vertical heat fluxes;
$R, R_c, R_{c\min}, R_c^{(s)}$,	Rayleigh numbers;
$R^*, R_c^*, R_{c\min}^*$,	Rayleigh numbers based on vertical parameters K_v, k_v ;
$T, T_a, T_c, T', T^{(i)}$,	temperatures;
$\Delta T, \Delta T_c$,	temperature differences across system;
u, u', w, w' ,	mass flux velocity components;
x, z ,	rectangular coordinates;
z_i ,	elevation of i th interface.

ρ, ρ_a ,	densities of saturating fluid;
σ ,	slope coefficient for Nusselt number;
$\psi, \psi^{(i)}$,	stream functions.

1. INTRODUCTION

IN A RECENT paper [1], an investigation was made of the convergence towards homogeneous anisotropy [2] for convection in a porous medium composed of alternating layers. When the number of layers increases, the layered configuration is able to be approximated increasingly better by a homogeneous model medium with a permeability tensor determined by the average horizontal and vertical permeabilities. However, this is true only for large-scale convection which penetrates all the layers. For local convection, which consists mainly of recirculations within the alternate more permeable layers, the anisotropic modelling is not suitable.

In ref. [1], a sufficient condition for local convection to be preferred was established, but not any general necessary condition. So far, then, there is no general criterion available for deciding whether the anisotropic modelling is useful. Detailed results were given only for the case of alternating layers of equal thicknesses. So the need for supplementary results is recognized. However, a study of all possible ratios of layer thicknesses and permeabilities would be too complicated and unreadable. Therefore the present paper is devoted to the limit case where one of the two alternating layers is very thin and has very small permeability. As in ref. [1], the methods of solution will be those developed previously [3, 4]. While in ref. [1] the case of layered thermal conductivity was also treated in detail, here layering in permeability only will be discussed.

Greek symbols

α ,	thermal expansion coefficient;
β ,	permeability ratio, K_2/K_1 ;
γ ,	thermal conductivity ratio, k_2/k_1 ;
ϵ ,	layer thickness ratio, $d_2/(d_1 + d_2)$;
ζ ,	perturbation parameter (in Appendix);
λ ,	'sheet' parameter, β/ϵ ;
ν ,	kinematic viscosity of saturating fluid;
ζ, ξ_0 ,	permeability anisotropy parameter, K_H/K_v ;

Special emphasis will be placed on the case of a constant-pressure upper boundary. This is because of its relevance to convection in snow layers [5, 6]. It has been suggested [7, p. 302] that snow layers may be represented as anisotropic with respect to thermal convection. The conditions will be determined under which this is true.

The case of impermeable boundaries is also of special interest in connection with insulation techniques. The destabilizing effects of thermal interaction through horizontal impermeable sheets placed within porous insulation materials will be investigated. The present study also has relevance to geothermal problems [8].

2. FORMULATION OF THE THIN LAYER LIMIT PROBLEM

Only the case of two alternating layer types, with an even total number of layers, will be studied. The notation of ref. [1] will be used. The general formulation of the physical problem is briefly recapitulated in the Appendix. It is now assumed that layer 2 (Fig. 15), representative of all even-numbered layers, has a very small thickness d_2 and a very small permeability K_2 . The aim is to investigate the limit case where both d_2 and K_2 tend to zero with the ratio K_2/d_2 kept at a certain finite value. Layer 2 then becomes what may be called a 'permeable sheet', or an 'impermeable sheet' in the special case $K_2 = 0$.

The limit $K_2, d_2 \rightarrow 0$ with K_2/d_2 fixed at a finite value is unique. This is most conveniently seen by noticing that the pressure drop in the fluid, on passing through layer 2, tends towards the value

$$\Delta p = vw \frac{d_2}{K_2}. \quad (1)$$

So, in the limit case, the pressure falls in the direction of movement through the sheet by an amount equal to a constant times the vertical velocity w . This may be taken as a dynamic boundary condition. The corresponding kinematic condition is that w is the same on both sides of the sheet. Mathematically, the configuration corresponds to a porous medium composed of layers of type 1 alone, interrupted by internal dynamic and kinematic boundary conditions (representing the sheets). So layer 2 is removed from the explicit analysis. This direct formulation of the limit problem asserts its uniqueness, as all limiting procedures have been removed.

However, this alternative method will not be applied in practice. The methods of McKibbin and O'Sullivan [3, 4], retaining layer 2 in the solution procedure, allow approach towards the limit with satisfactory accuracy.

Mathematically, the passage to the limit case $K_2, d_2 \rightarrow 0$ with K_2/d_2 finite is a reduction from a problem with two independent layering parameters K_2/K_1 and d_2/d_1 to a one-parameter problem; the relevant parameter λ will be introduced below. In ref. [1], a one-parameter was obtained in another way, by keeping d_2/d_1 equal to 1.

Now the convergence towards the thin layer limit will be discussed. Some new notation is needed for this purpose. The relative layer thickness ratio $d_2/(d_1 + d_2)$ is denoted by ε . (This is just a matter of convention; in order to study the limit case $K_2, d_2 \rightarrow 0$, ε might equally well have been chosen as d_2/d_1 .) As in ref. [1], the permeability ratio K_2/K_1 is denoted by β , and a new 'sheet parameter' λ is introduced, defined by

$$\lambda = \frac{\beta}{\varepsilon} = \frac{K_2/K_1}{d_2/(d_1 + d_2)}. \quad (2)$$

The limit case corresponds to both ε and β tending to zero. For a given value of λ , the problem is to choose a value of the relative thickness ε which is small enough so that the thin layer problem is converged. The corresponding small value of β is given by

$$\beta = \lambda \varepsilon. \quad (3)$$

The average horizontal and vertical permeabilities may now be expressed as

$$K_H = (1 - \varepsilon + \lambda \varepsilon^2) K_1, \quad (4)$$

$$K_V = (1 - \varepsilon + \lambda^{-1})^{-1} K_1. \quad (5)$$

The permeability anisotropy parameter ξ is then given by

$$\xi \equiv K_H/K_V = (1 - \varepsilon + \lambda \varepsilon^2) \left(1 - \varepsilon + \frac{1}{\lambda} \right). \quad (6)$$

By its definition, $\varepsilon = d_2/(d_1 + d_2)$ is confined between 0 and 1. Figure 1 shows the anisotropy parameter ξ as a function of ε for some values of the sheet parameter λ , as

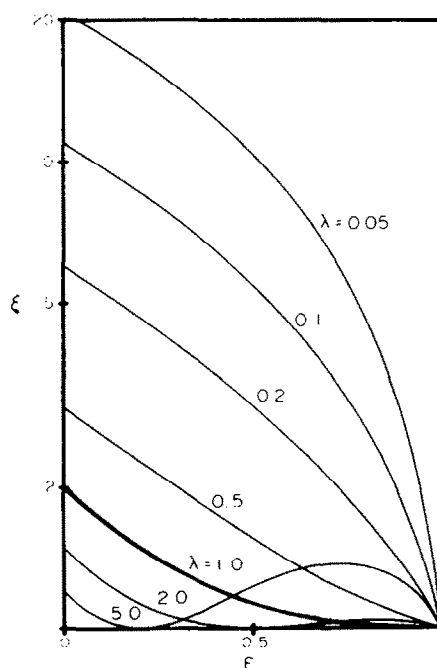


FIG. 1. Permeability anisotropy parameter ξ as a function of layer thickness ratio $\varepsilon = d_2/(d_1 + d_2)$, for various values of the sheet parameter $\lambda = \beta/\varepsilon = (K_2/K_1)/\varepsilon$, calculated from equation (6).

given by equation (6). When $\varepsilon \rightarrow 0$, ξ tends towards the limiting value ξ_0 given by

$$\xi_0 = 1 + \frac{1}{\lambda}. \quad (7)$$

The deviation from this value when ε is non-zero is given by

$$\xi - \xi_0 = -\left(2 + \frac{1}{\lambda}\right)\varepsilon + (2 + \lambda)\varepsilon^2 - \lambda\varepsilon^3. \quad (8)$$

Since only small values of ε are of interest, powers of ε higher than the first can be neglected. To this approximation, the relative error in the anisotropy parameter ξ is

$$\frac{\xi - \xi_0}{\xi_0} = -\frac{2\lambda + 1}{\lambda + 1}\varepsilon. \quad (9)$$

The magnitude of this relative error changes only slowly with the sheet parameter λ and lies between ε and 2ε . When $\lambda = 1.0$,

$$\left|\frac{\xi - \xi_0}{\xi_0}\right| = \frac{3}{2}\varepsilon,$$

which is just in the middle of its range of variation. So this value of λ emerges as a representative choice for investigating the convergence of the flow problem with respect to the relative thickness ε , as ε tends towards zero.

Figures 2–4 show this convergence for $\lambda = 1.0$, corresponding to $\xi_0 = 2.0$. Figure 2 represents the case of an impermeable upper boundary ('closed top'), while Figs. 3 and 4 show results for a constant-pressure upper boundary ('open top'). Throughout this paper the lower boundary is assumed impermeable and both upper and lower boundaries are maintained at uniform temperatures. Figure 3 represents the case where the thin layer is at the top while Fig. 4 gives results for the thick layer at the top. (For the closed top case, there is no quantitative difference between results for thin or thick layer on top, owing to symmetry.) In each figure, ξ varies between 1 and 1.97.

In Figs. 2–4, each of (a), (b) and (c) show respectively the critical Rayleigh number $R_{c\min}^*$, the corresponding cell-width L_c and the slope parameter σ (see Appendix) for the heat transfer, as functions of the relative thickness ε for different numbers of layers, N . In Fig. 4, ε

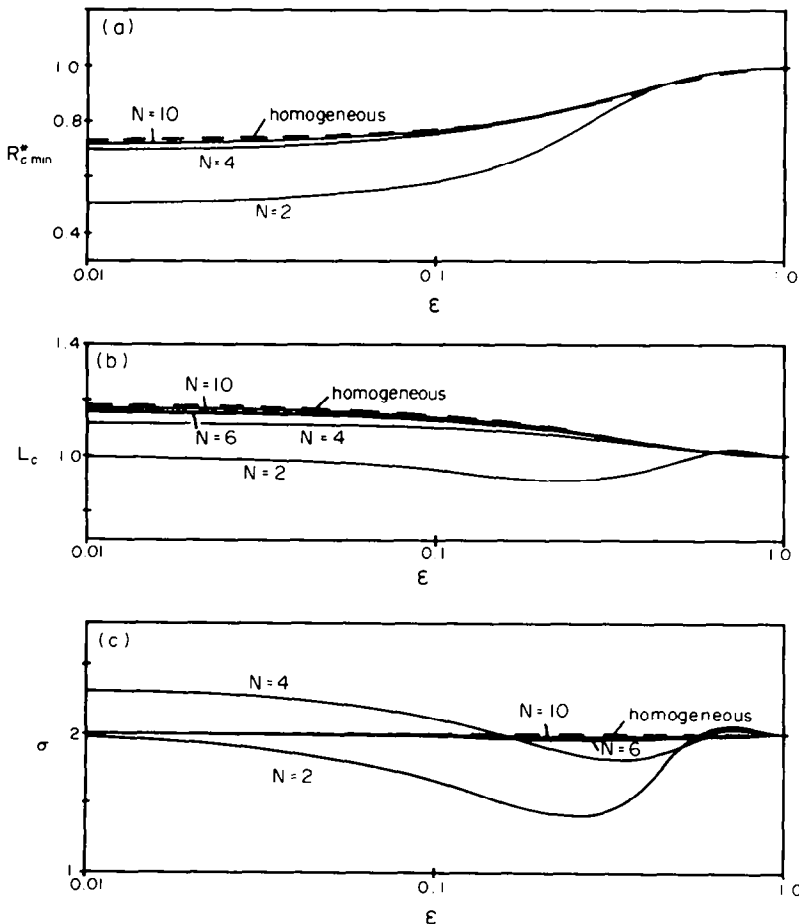


FIG. 2. Variation of critical Rayleigh number $R_{c\min}^*$, cell-width L_c and corresponding values of the Nusselt number slope parameter σ , with the layer thickness ratio ε for the closed top case, when sheet parameter $\lambda = 1.0$. (a) $R_{c\min}^*$ vs ε ; (b) L_c vs ε ; (c) σ vs ε .

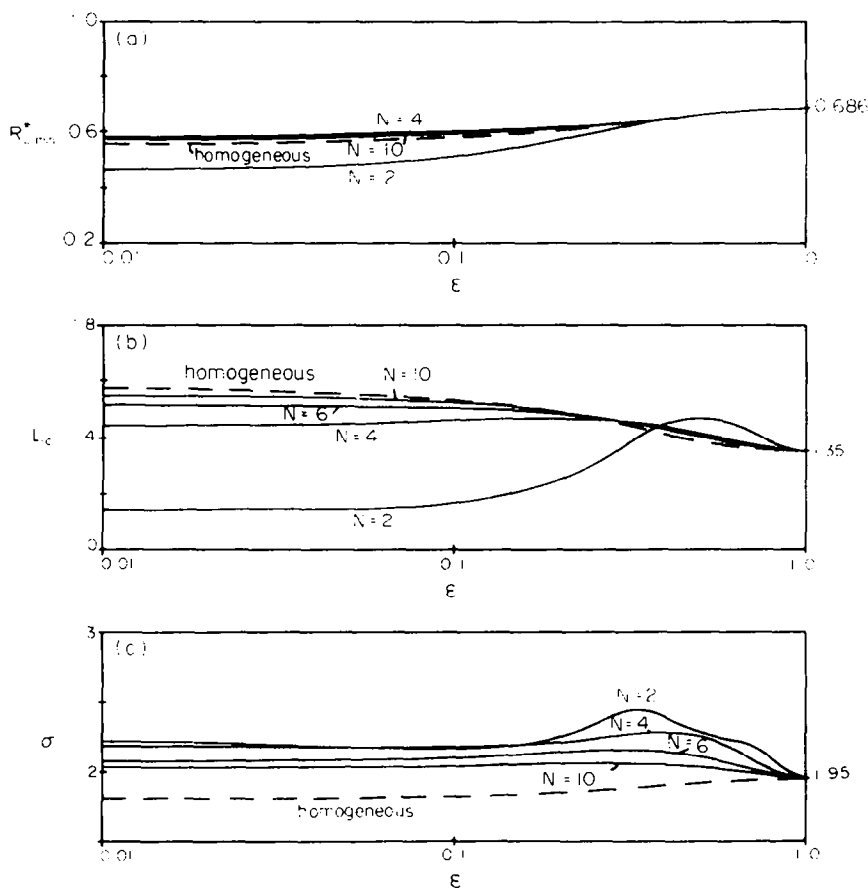


FIG. 3. Variation of R_{cmin}^* , L_c and corresponding values of σ with ϵ for the open top case where the thin layer is on top, when $\lambda = 1.0$. (a) R_{cmin}^* vs ϵ ; (b) L_c vs ϵ ; (c) σ vs ϵ .

and the sheet parameter λ are redefined and marked with primes because layer 1 is the thin one instead of layer 2. All of the curves in Figs. 2–4 tend to become horizontal lines near $\epsilon = 0.01$, while their behaviour for larger values of ϵ may be quite complicated. The true asymptotic limits as $\epsilon \rightarrow 0$ are known only for $N = 2$, for the closed top case and for the open top case with the thick layer at the top. These values are found in ref. [1], and are as follows: for a closed top, limits are $R_{cmin}^* = 0.5$, $L_c = 1.0$ and $\sigma = 2.0$; for an open top with the thick layer at the top, $R_{cmin}^* = 0.343$, $L_c = 1.35$ and $\sigma = 1.95$. The convergence towards these known limits is satisfactory for $\epsilon = 0.01$. Note the reduction of the Rayleigh numbers given in ref. [1] by the factor $\frac{1}{2}$. This is due to the fact that K_H is the relevant permeability in these asymptotic problems which are essentially one-layer problems, while K_V is the permeability which enters the definition of R^* . So $\xi_0 = K_H/K_V = 2.0$ gives the factor $\frac{1}{2}$.

Generally the value $\epsilon = 0.01$ will be used in numerical investigations of the thin layer limit. Although results for convergence have been presented only for $\lambda = 1.0$, some further results given below will check the convergence for other values of the sheet parameter λ . For example, Fig. 9 will show that the

convergence is satisfactory for the case when λ tends to zero.

3. RESULTS AND DISCUSSION

Some results will now be presented for the thin layer limit, obtained by choosing the relative thickness $\epsilon = 0.01$. An investigation of the convergence towards homogeneous anisotropy [2] is displayed in Figs. 5–7. They represent, respectively, the cases of closed top, open top with the thin layer at the top, and open top with the thick layer at the top. These figures should be compared with Fig. 12 of the present authors' previous paper [1]. Figures (a) show the critical Rayleigh number R_{cmin}^* . Upper bounds for the onset of local convection are not displayed as there is a separate figure (Fig. 8) for that purpose. The sufficient condition for onset of local convection in a closed top system [1, equation (6.1)] still holds here in the relevant case represented by Fig. 5(a). In the limit $\epsilon \rightarrow 0$, this condition can be rearranged to give a bound for the sheet parameter, as

$$\lambda < \frac{1}{N(N-2)}. \quad (10)$$

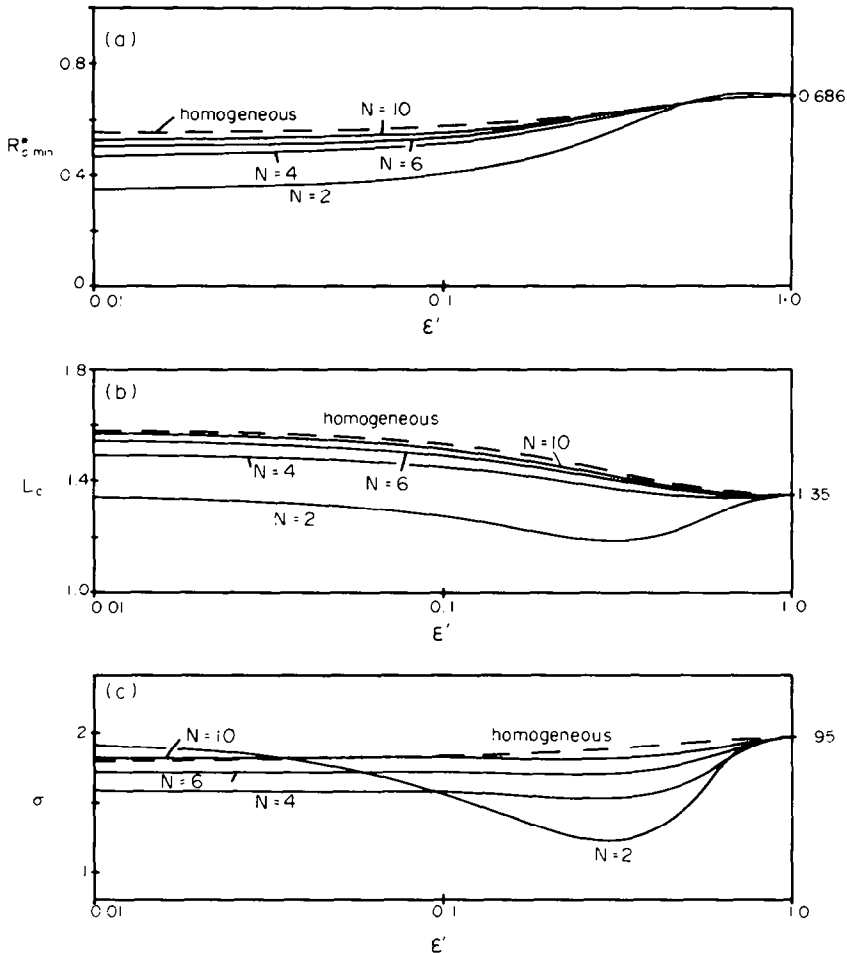


FIG. 4. Variation of $R_{c,min}^*$, L_c and corresponding values of σ with $\epsilon' = d_1/(d_1 + d_2)$ for the open top case where the thick layer is on top, when $\lambda' = (K_1/K_2)/\epsilon' = 1.0$. (a) $R_{c,min}^*$ vs ϵ' ; (b) L_c vs ϵ' ; (c) σ vs ϵ' .

or, in terms of anisotropy,

$$\xi > (N-1)^2. \quad (11)$$

These two equivalent inequalities describe conditions under which local convection must be preferred when permeable sheets are distributed in a porous medium. (It may also occur outside this range.)

It was indicated in ref. [1] that an even number of alternating layers gives the best convergence towards homogeneous anisotropy. Expressed in terms of periods of layering, only complete periods should be present within the boundaries in order to obtain optimal convergence. This is confirmed by the present analysis. It may be demonstrated clearly from Figs. 5(a) and 7(a), because the thin layer limit cases of N layers treated there cover $N-1$ layers as well. This is because one sheet is without significance, namely the one in contact with an impermeable boundary. But although it does not influence the flow, it is to be included to keep N as an even number [in order that the definitions (4)–(6) may be retained]. Actually, if the results of Figs. 5(a) and 7(a) are presented in terms of $N-1$ layers (odd

number) instead of N layers (even number), the convergence towards anisotropy is much poorer.

Figures (b) in Figs. 5–7 show the critical cell-widths L_c . Their variation with the anisotropy parameter ξ is smoother than for equal layer depths [1, Fig. 12(b)] and their asymptotic values for strong anisotropy are much larger. This is because, for given N and large ξ , the layers in which local convection takes place are twice as thick as in the case of equal layer depths, and the near-square cells consequently have larger cell-widths. One reason for the more smooth transition is that two neighbouring regions of local convection are much closer together than in the case of equal layer depths. Interactions through the sheets tend to give a smoother transition from large-scale to local convection. However, the transition towards local convection (and breakdown of the anisotropic modelling) sets in for weaker anisotropy than for equal layer depths. This is because the relevant local Rayleigh numbers are four times as large in the thin-layer limit: each more permeable layer has twice the thickness and twice the temperature difference of the corresponding layer in the case of equal layer depths.

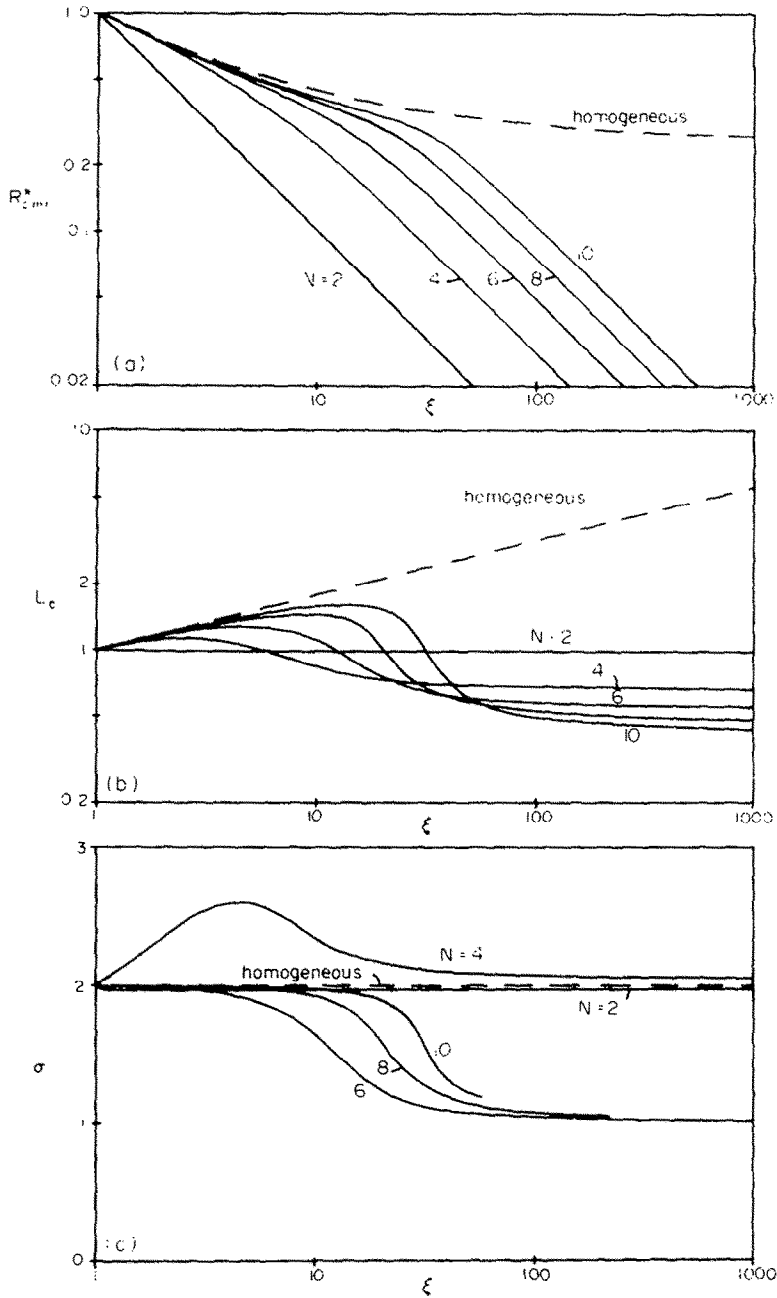


FIG. 5. Variation of $R_{c,min}^*$, L_c and corresponding values of σ with ξ for the closed top case, when $\epsilon = 0.01$. Values are given for $N = 2, 4, 6, 8, 10$ and the homogeneous system. (a) $R_{c,min}^*$ vs ξ ; (b) L_c vs ξ ; (c) σ vs ξ .

Figures (c) in Figs. 5-7 show the Nusselt number slope parameter σ as a function of ξ for different numbers of layers, and also the values for homogeneous anisotropy. As stated in the Appendix, σ is defined by the straight line approximation to the Nusselt number Nu , valid for slightly supercritical Rayleigh numbers, and given by

$$Nu = 1 + \sigma(R/R_c - 1) = 1 + \sigma(\Delta T/\Delta T_c - 1). \quad (12)$$

The values of σ given relate to the critical cell-width L_c .

For the homogeneous anisotropic medium with a

closed top, analytical results from Kvernvoid and Tyvand [2] are

$$R_{c,min}^* = \frac{1}{4}(1 + \xi^{-1/2})^2, \quad (13)$$

$$L_c = \xi^{1/4}, \quad (14)$$

$$\sigma = 2.0. \quad (15)$$

These are represented by the broken curves in Fig. 5. The corresponding broken curves for the open top case in Figs. 6 and 7 are based on numerical calculations in McKibbin and Tyvand [1, Table 1].

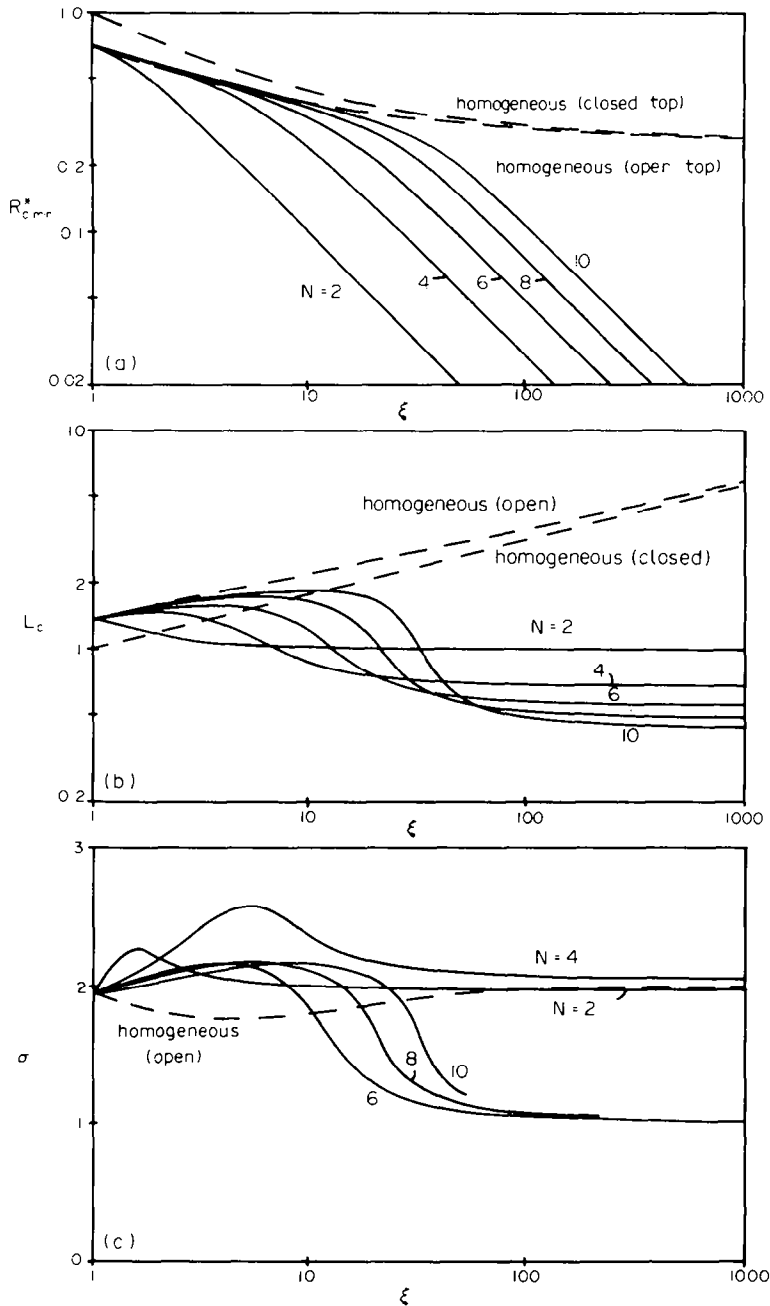


FIG. 6. Variation of $R_{c,min}^*$, L_c and corresponding values of σ with ξ for the open top case where the thin layer is on top, when $\varepsilon = 0.01$. Values are given for $N = 2, 4, 6, 8, 10$ and the homogeneous system. (a) $R_{c,min}^*$ vs ξ ; (b) L_c vs ξ ; (c) σ vs ξ .

For the numbers of layers displayed in Figs. 5–7, i.e. up to $N = 10$, convergence towards homogeneous anisotropy is found only in the cases of closed top and open top with the thick layer on the top. The other case, open top with the thin layer on the top, does not give a purely open top boundary condition for the system as a whole. As will be seen from the streamline patterns of Figs. 11 and 13, this gives considerable recirculation even for a large-scale convection, while ordinarily most of the fluid is convected out of the porous medium when there is an open-top boundary condition [10]. The

sheet on the top partly 'closes' the boundary—there is effectively a tendency towards the closed top, this tendency being slight for weak anisotropy but increasing rapidly with ξ . In total, the case of an open top with the sheet on top gives a smooth transition from a truly open top for $\xi = 1$ to an effectively closed top as $\xi \rightarrow \infty$. The fact that a true convergence towards homogeneous anisotropy is not found when the sheet is on the top is also apparent from Figs. 3(a) and (c), 6(a) and especially Fig. 6(c). In this last figure hardly any convergence towards anisotropy is seen at all. In the

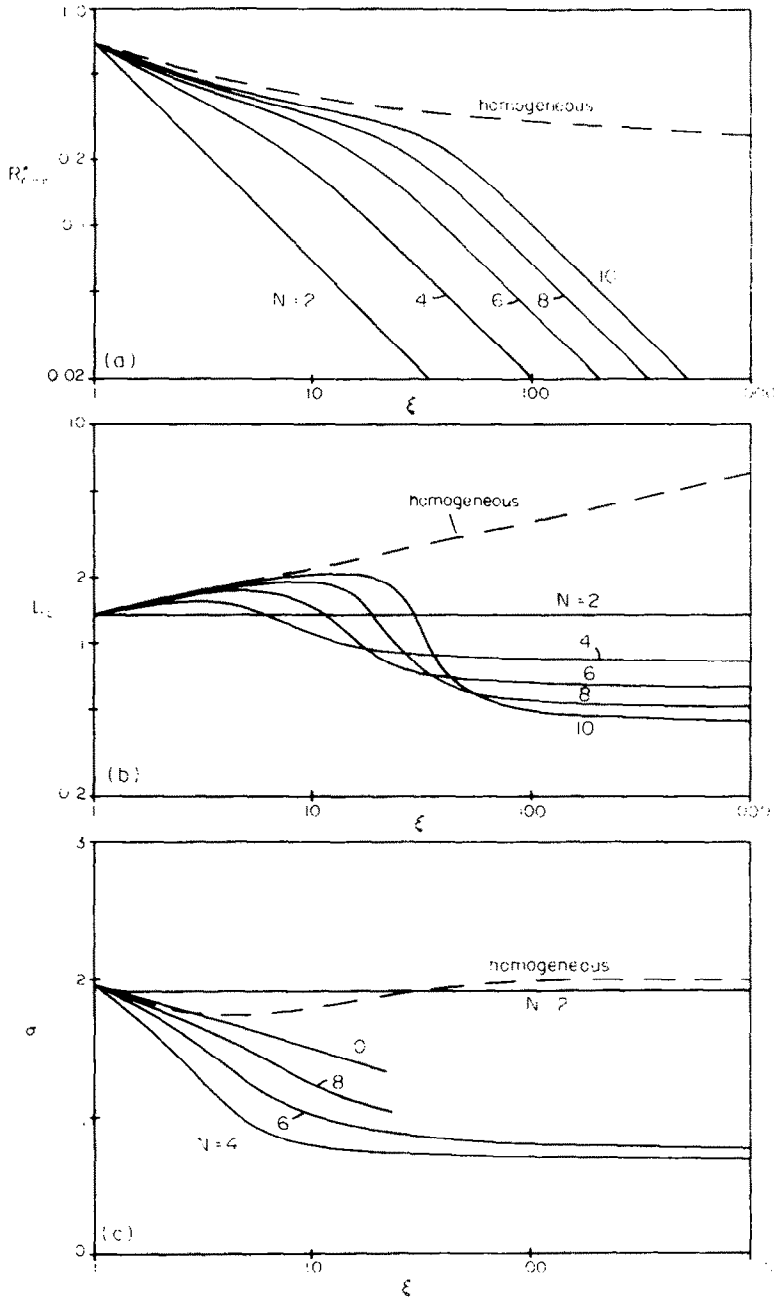


FIG. 7. Variation of $R_{c,min}^*$, L_c and corresponding values of σ with ξ for the open top case where the thick layer is on top, when $\varepsilon' = 0.01$. Values are given for $N = 2, 4, 6, 8, 10$ and the homogeneous system. (a) $R_{c,min}^*$ vs ξ ; (b) L_c vs ξ ; (c) σ vs ξ .

corresponding case of the thick layer at the top [Fig. 7(c)] there is a convergence towards homogeneous anisotropy as N increases, although it is somewhat weaker than in the closed top case [Fig. 5(c)].

Figure 8 shows the critical values of the Rayleigh number R defined in terms of the permeability K_1 (or alternatively, R' defined in terms of K_2 when layer 2 is the thick one) as a function of ξ for different numbers of layers. Figures 8(a), (b) and (c) just repeat the results of Figs. 5(a), 6(a) and 7(a) respectively, but in slightly

different form. However, only by referring to Fig. 8 can the stabilizing effects of inserting impermeable sheets within an otherwise homogeneous material be studied. There are always constant asymptotic values of R_c corresponding to impermeable sheets ($\xi \rightarrow \infty$). These values increase with increasing N . It is easy to find upper bounds for these values. Obvious general upper bounds are

$$R_c = \left(\frac{N}{2}\right)^2, \quad N = 2, 4, \dots, \quad (16)$$

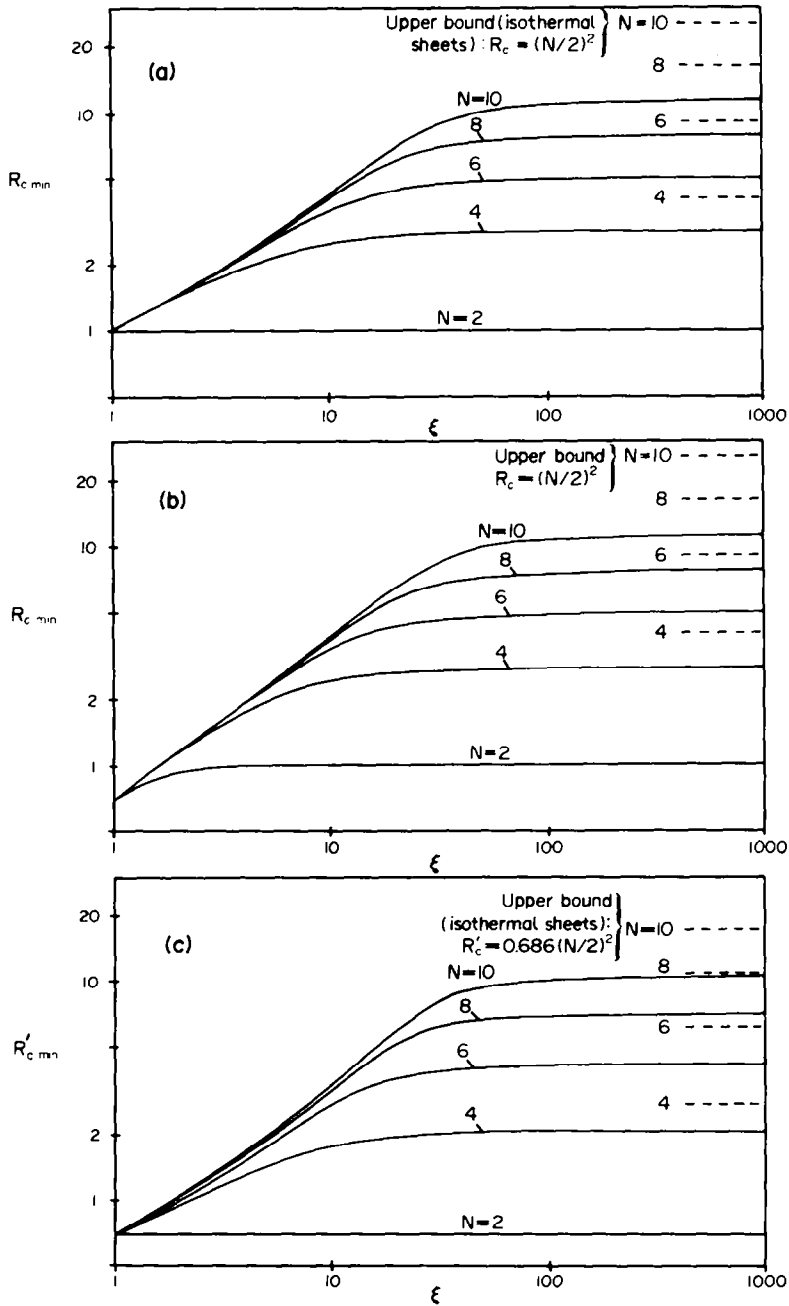


FIG. 8. Variation of $R_{c,min}$, the Rayleigh number defined in terms of the permeability of the thicker layer(s), with ξ for $N = 2, 4, 6, 8$ and 10 . Upper bounds determined by equations (16) and (17), as appropriate, are also marked. (a) Closed top; (b) open top with thin layer on top; (c) open top with thick layer on top.

corresponding to onset of local convection in a single layer if the boundaries are impermeable and perfectly heat-conducting (and hence isothermal). Equation (16) gives upper bounds because thermal interaction as well as permeability of boundaries act in a destabilizing fashion [1, 9]. For the case of the open top with the thick layer on top it is possible to find improved upper bounds, namely

$$R'_c = 0.686 \left(\frac{N}{2} \right)^2, \quad N = 2, 4, \dots \quad (17)$$

This corresponds to onset of local convection in a single layer with both boundaries isothermal, but with the upper one open while the lower one is impermeable. The numerical value in equation (17) is taken from McKibbin and Tyvand [1, Table 1], but the problem has been solved earlier (see ref. [11], for example).

Figures 9 and 10 show streamlines and isotherms representing asymptotically the case of impermeable sheets. They have been calculated for the sheet parameter $\lambda = 0.001$, corresponding to anisotropy

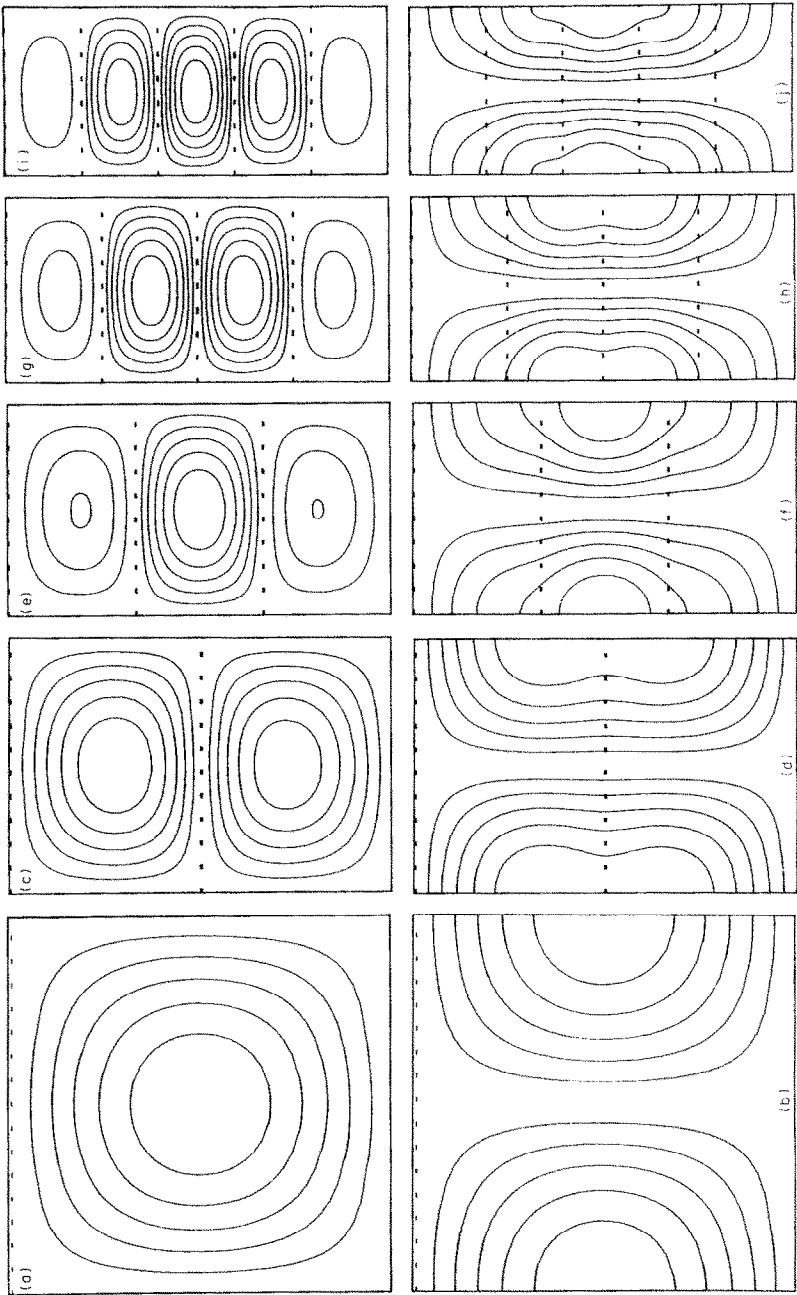


FIG. 9. Streamlines and isotherms at onset of convection for the closed top case where $\varepsilon = 0.01$ and $\lambda = 0.001$, representing the asymptotic case of impermeable sheets. (a), (b) $N = 2 (R_{cmin} = 1.01, L_c = 0.99)$; (c), (d) $N = 4 (2.80, 0.67)$; (e), (f) $N = 6 (4.97, 0.56)$; (g), (h) $N = 8 (7.75, 0.49)$; (i), (j) $N = 10 (11.1, 0.44)$.

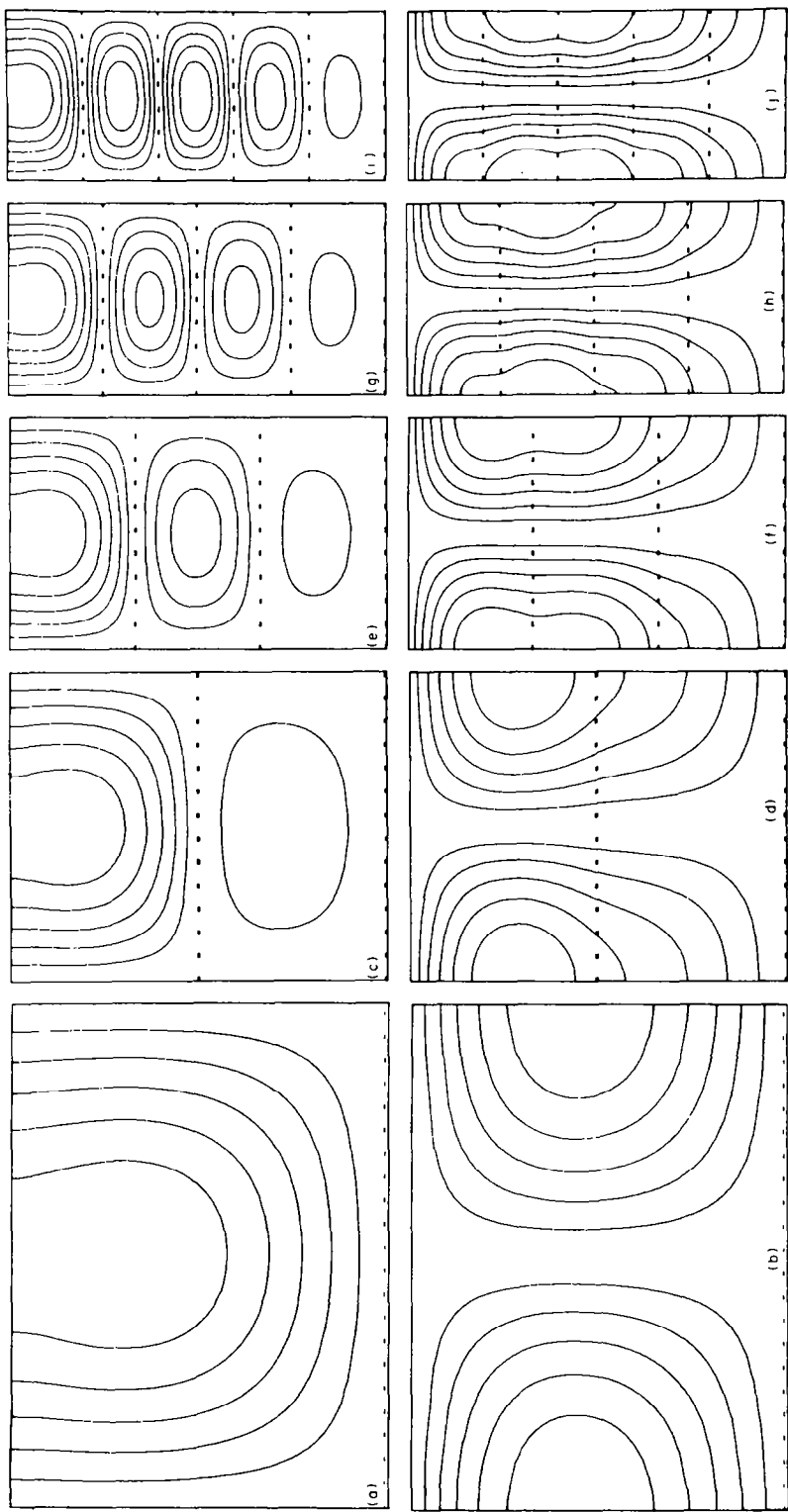


FIG. 10. Streamlines and isotherms at onset of convection for the open top case where the thick layer is on top and where $\varepsilon' = 0.01$ and $\lambda' = 0.001$, representing the asymptotic case of impermeable sheets. (a), (b) $N = 2$ ($R_{c\min} = 0.694$, $L_c = 1.34$); (c), (d) $N = 4$ (2.08, 0.83); (e), (f) $N = 6$ (4.23, 0.61); (g), (h) $N = 8$ (7.07, 0.51); (i), (j) $N = 10$ (10.6, 0.44).

$\xi = 991$, and layer permeability ratio $\beta = 10^{-5}$. (The isotherms indicate equally spaced temperature departures from the preconvection conductive state.) The streamlines are all practically closed within each layer with no penetration of fluid through the sheets between the layers. So all information about the motion in neighbouring layers must be transmitted by thermal interactions.

Figure 9 represents the closed top case. In the thin layer limit, the streamline patterns are symmetric about $z = d/2$, due to the symmetric boundary conditions. This makes it possible to control the convergence towards the thin layer limit for the choice of the relative thickness ratio $\varepsilon = 0.01$. Only in Fig. 9(e) is a slight asymmetry found for the inner streamlines of the upper and lower thick layers. Generally, the symmetry of the streamlines in Fig. 9 indicates that the choice $\varepsilon = 0.01$ gives good convergence for the case of small values of the sheet parameter λ . In this symmetric configuration, the thick layer(s) nearest the middle are always the most active one(s). This is because thermal interactions between the layers act in a destabilizing manner.

The case of an open top with the thick layer on top is represented by Fig. 10. There is a substantial asymmetry in the kinematic boundary conditions which makes all streamline and isotherm patterns asymmetric. Although purely mechanical in origin, this asymmetry must be transmitted through the sheets solely by thermal interactions, because no mechanical interactions are possible. In this case the thick layer nearest to the middle is not the most active one. The uppermost layer has the direct destabilizing effect of the open top, compared to the other thick layers which have effectively closed tops. The open-top effect in the uppermost layer turns out to be stronger than the favouring of onset of convection in the inner layers due to thermal interactions. So the top layer is always the most active one. Even so, the difference in activity of the other layers is not very large for $N = 10$, where the second and third thick layers from above are almost equally active.

It has already been mentioned that thermal interactions between neighbouring layers act in a destabilizing way and that they may also transmit kinematic information indirectly. These interactions also give preference for the flow to begin more strongly near an internal sheet rather than near the upper and lower boundaries of uniform temperatures. This is perhaps most easily seen from Fig. 9(c).

However, the strongest effect of thermal interactions are on the isotherms shown in Figs. 9 and 10. They are not similar to the streamlines (i.e. closed within each layer) as they would have been if the sheets were perfectly heat-conducting, thereby preventing thermal interactions. Conversely, the isotherms penetrate all layers, with characteristic changes of curvature about each sheet. Apart from this, their shapes are not very different from the homogeneous case, even for local convection.

The case of open top with the thin layer at the top has

not been displayed for the limit case of impermeable sheets. This is because it is effectively the same as the closed top case. However Fig. 11 shows a full transition from a homogeneous isotropic medium to a medium interrupted by effectively impermeable sheets, for the open top case with the thin layer at the top. Only the case of six layers is studied, with ξ varying from 1 to 991. Three equally spaced sheets are introduced into a homogeneous medium. In Figs. 11(a) and (b) these sheets have the same permeability as the surroundings, so the medium is still homogeneous. For each subsequent pair of figures (streamlines and isotherms) the permeability of these sheets is reduced by a factor of 10. So a gradual closing of the internal boundaries or sheets as well as a closing of the top are observed simultaneously. A strong recirculation of the flow is present even for $\xi = 2.0$ ($\lambda = 1.0$) in Fig. 11(e). This is shown further in Fig. 13.

Streamline patterns at the onset of convection are shown in Figs. 12-14 for all three types of configuration with the number of layers varying from 2 up to 10, for the case $\xi = 2.0$ ($\lambda = 1.0$). Figures 12, 13 and 14 represent closed top, open top with the thin layer at the top and open top with the thick layer at the top, respectively. In all these cases, large-scale convection occurs. As the study above has shown, the case of open top with the thin layer at the top lies between the two other cases. The most important difference between Figs. 13 and 14 is that there is a much stronger recirculation in the first case.

4. APPLICATIONS TO CONVECTION IN SNOW LAYERS AND INSULATION TECHNIQUES

In connection with snow layers, the upper boundary condition of constant pressure (open top) will be applied. The 'sheets' of low permeability here correspond to thin icy layers formed in brief periods of melting and re-freezing. Such layers are often present in old snow. The investigation of an anisotropic description of convection in layered snow may be made without first taking into account the transport of water vapour, which is discussed by Palm and Tveitereid [5]. The present results are restricted to alternating layers of ice and snow with equal distances between the ice layers, but have some relevance for more general cases also.

It has been found above that equal numbers of ice and snow layers must be taken into account in the definition of an average anisotropic permeability, even if the physical situation does not exhibit equal numbers. If so, one of the layers must be excluded from the definition of anisotropy.

It has also been found that convergence towards homogeneous anisotropy is not good in the case of an ice layer on the top. This is because recirculation is less pronounced in the anisotropic model with the same open-top boundary condition [10]. The anisotropic model may have to be rejected for cases where an ice layer is on top when the recirculation is qualitatively

important. This is relevant to the transport of water vapour: for melting, it is crucially important whether the vapour recirculates or is transported out of the snow. Nevertheless, the quantitative agreement between the critical Rayleigh number for the layered case and the corresponding value for anisotropy is satisfactory for large-scale convection [Fig. 6(a)]. However the heat transport [Fig. 6(c)] can never be described in terms of anisotropy when the ice layer is on top.

When a snow layer is on the top, the anisotropic modelling is qualitatively more correct because recirculation is weak for large-scale convection. A true, although slow, convergence towards homogeneous anisotropy is found. It is slow due to the strong activity in the uppermost layer – this activity will always be underestimated in the anisotropic model. So, when the number of layers is not very large, even large-scale convection will start considerably earlier (i.e. for lower Rayleigh number) and with smaller cell-width than in the anisotropic model. Paradoxically, the critical Rayleigh number for homogeneous anisotropy will (for $N \leq 10$) predict the case of ice layer on top better than the case of snow layer on top.

The present results may also have many applications to insulation techniques [12]. One aspect will be

concentrated on here, namely the introduction of equally spaced impermeable sheets in a homogeneous isotropic material confined between impermeable isothermal horizontal planes. Results for this case are shown in Fig. 8(a), which refers to the case where the sheets have the same thermal conductivity as the insulation material. The asymptotic critical temperature differences (as $\xi \rightarrow \infty$, $\lambda \rightarrow 0$) are approximately 2.8, 5.0, 7.8 and 11.2 times as large as for a homogeneous layer for 1, 2, 3 and 4 internal sheets respectively. So the insulating effect of these sheets is clear. The effect increases with the number of sheets, although the relative gain is reduced each time the number of sheets increases. If the sheets were not equally spaced, this increase in critical temperature differences would usually be smaller. However, thermal interactions reduce the critical temperature differences obtained when compared to the case of perfectly heat-conducting sheets. In the limit case for the latter sheet type, the critical temperature differences would be 4, 9, 16 and 25 times as large as for the homogeneous material for 1, 2, 3 and 4 internal sheets respectively. So it may be thought that metal foils should be inserted into insulation materials. However in practical applications, uneven heating at the boundaries would remove much of the advantage, because there would then be a strong

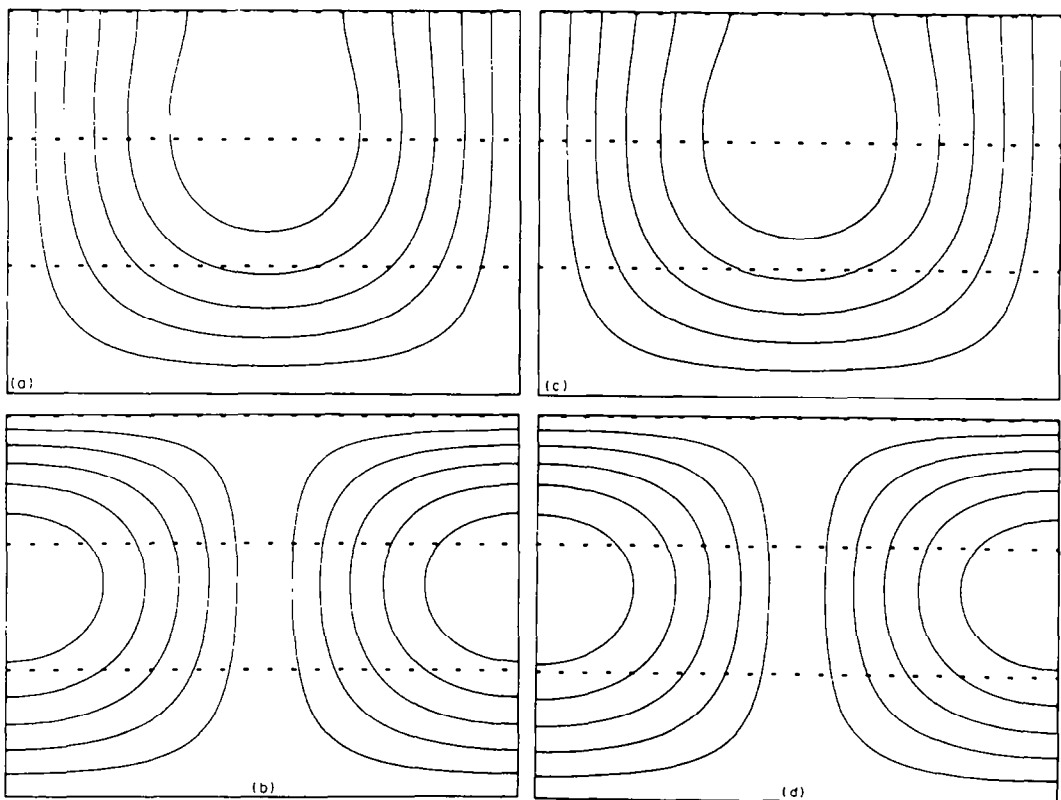
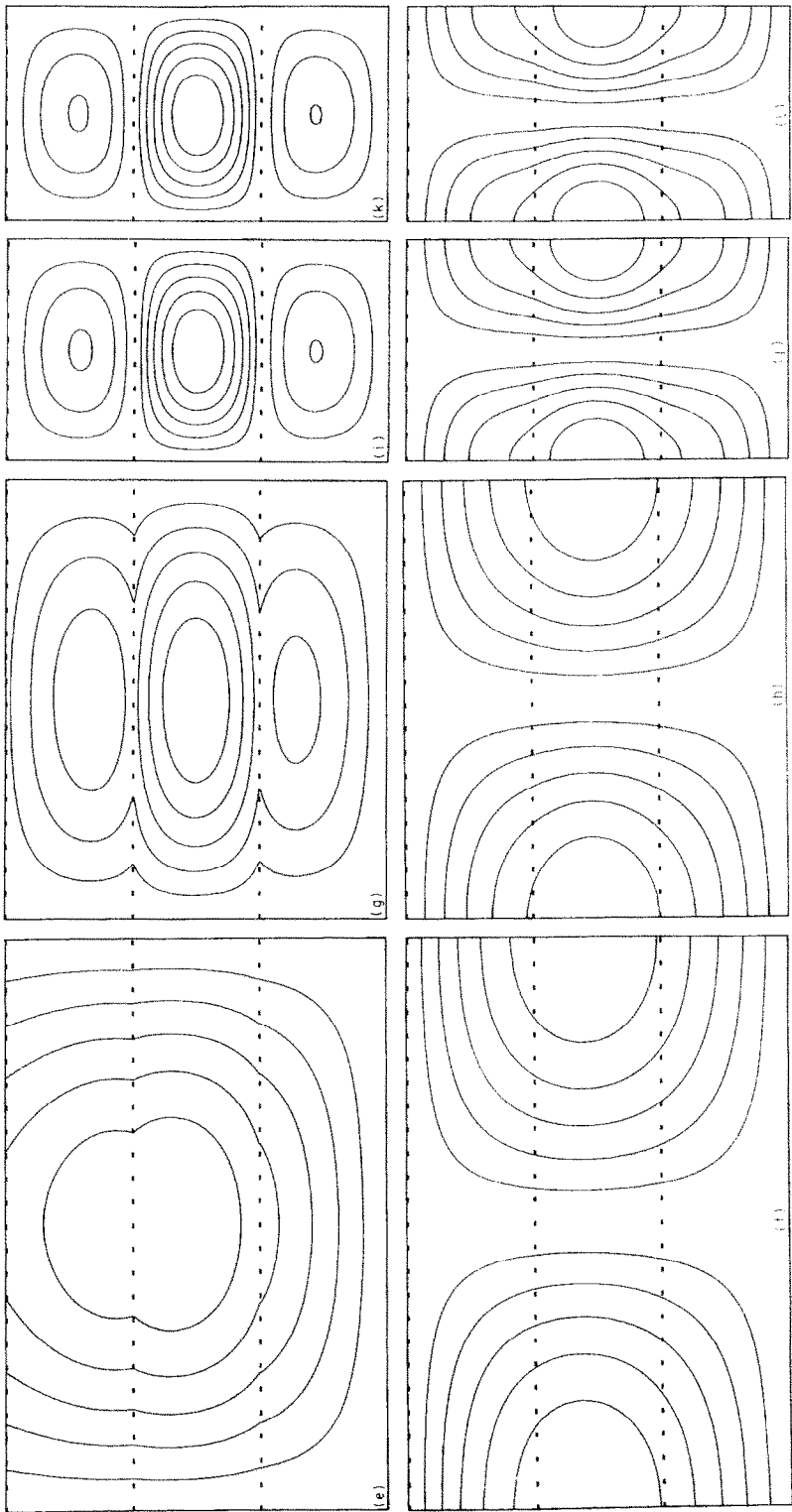


FIG. 11. Streamlines and isotherms at onset of convection for the open top case $N = 6$, $\varepsilon = 0.01$, where the thin layer is on top. The permeability of the sheets is reduced by a factor of 10 for each pair of figures subsequent to the first. (a), (b) $\beta = 1.0$, $\xi = 1.0$; (c), (d) $\beta = 0.1$, $\xi = 1.08$; (e), (f) $\beta = 0.01$, $\xi = 1.97$; (g), (h) $\beta = 0.001$, $\xi = 10.9$; (i), (j) $\beta = 10^{-4}$, $\xi = 100$; (k), (l) $\beta = 10^{-5}$, $\xi = 991$.

FIG. 11 – continued overleaf

FIG. 11—continued



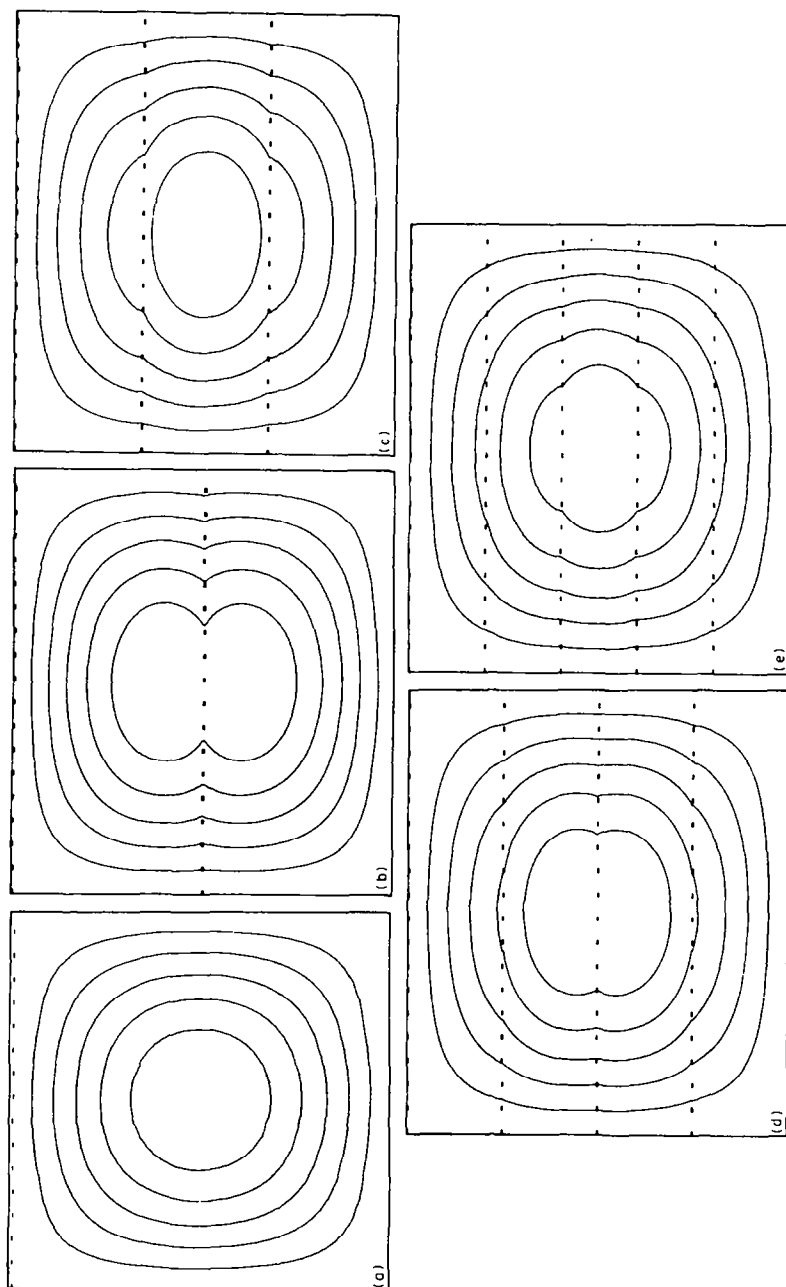


FIG. 12. Streamlines at onset of convection for the closed top case where $\varepsilon = 0.01$, $\lambda = 1.0$ ($\beta = 0.01$), (a) $N = 2$ ($R_{\text{crit}} = 1.01$, $L_c = 0.99$, $\sigma = 1.97$); (b) $N = 4$ (1.40, 1.12, 2.31); (c) $N = 6$ (1.43, 1.15, 1.99); (d) $N = 8$ (1.44, 1.17, 2.00); (e) $N = 10$ (1.45, 1.17, 2.00).

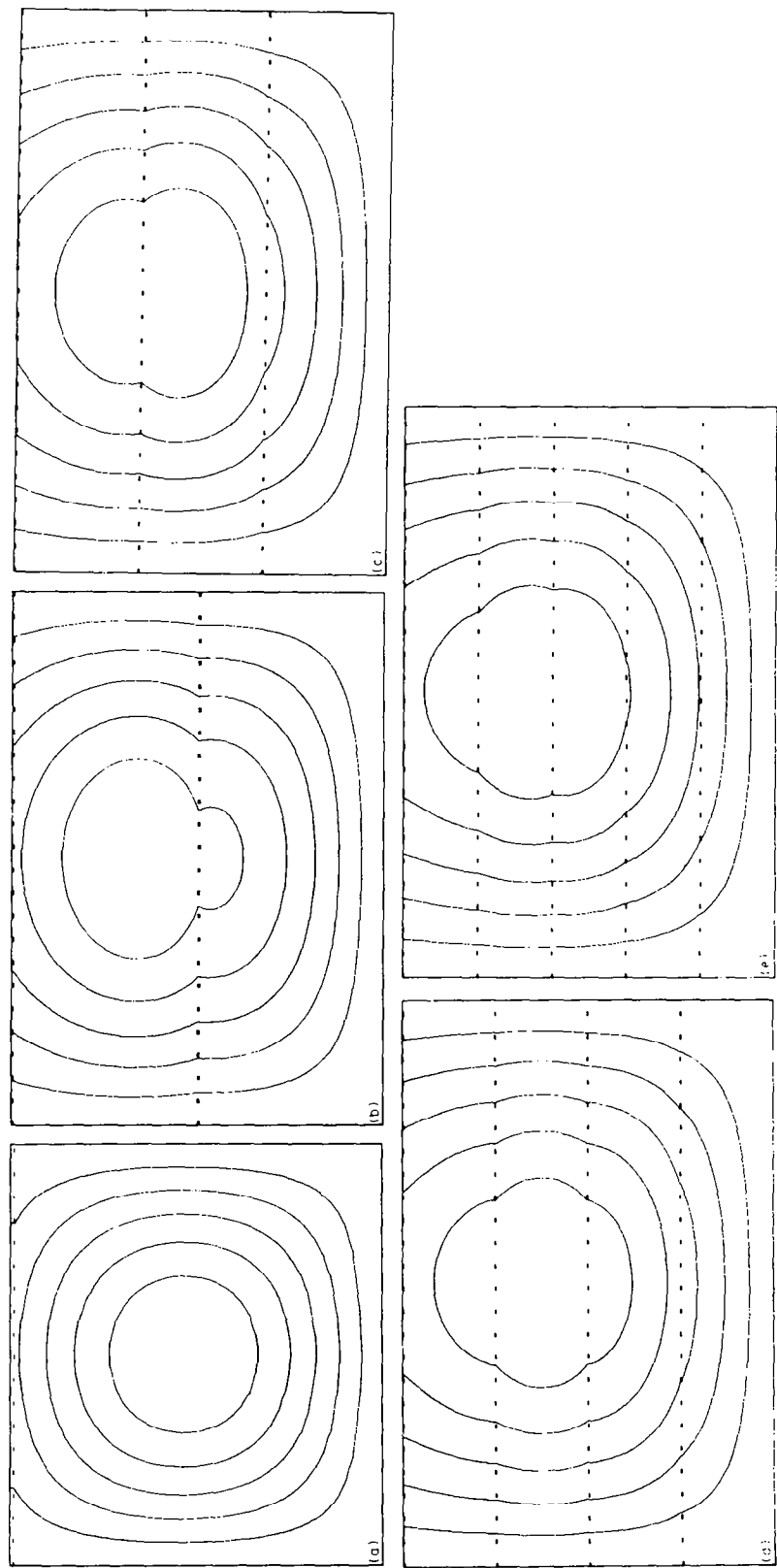


FIG. 10. Streamlines at onset of convection for the open top case where the thin layer is on top and where $\alpha = 0.01$, $\beta = 1.0$. (a) $N = 2$ ($R_{\text{crit}} = 0.919$, $L_c = 1.14$, $\sigma = 2.22$); (b) $N = 4$ (1.15, 1.45, 2.19); (c) $N = 6$ (1.15, 1.51, 2.08); (d) $N = 8$ (1.15, 1.54, 2.05); (e) $N = 10$ (1.14, 1.55, 2.03); (f) $N = 12$ (1.14, 1.55, 2.03).

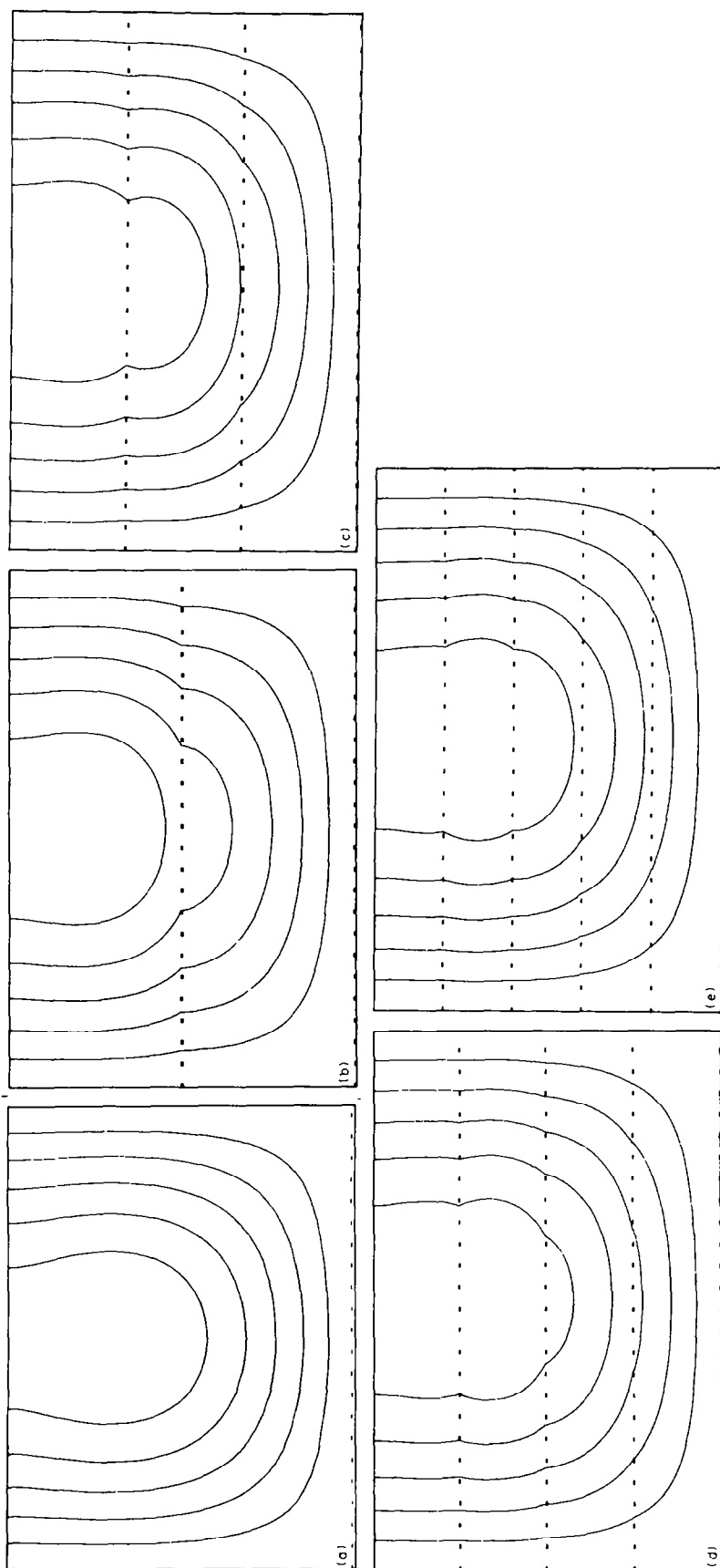


FIG. 14. Streamlines at onset of convection for the open top case where the thick layer is on top and where $\varepsilon' = 0.01$, $\beta = 1.0$ (a) $N = 2$ (0.941, 1.49, 1.58); (b) $N = 4$ (0.941, 1.49, 1.58); (c) $N = 6$ (1.00, 1.54, 1.72); (d) $N = 8$ (1.03, 1.56, 1.78); (e) $N = 10$ (1.05, 1.57, 1.82).

unwanted horizontal heat transport. Nevertheless, in problems with radiation loss, a metal foil might be advantageous by its action as a radiation shield.

The average heat flux subsequent to onset of convection is measured by the parameter σ . From Figs. 5(c) and 6(c) it is seen that for large values of the anisotropy parameter ξ , corresponding to small values of the sheet parameter λ , σ is smaller than the homogeneous values provided $N \geq 6$. When there is only one internal sheet ($N = 4$), convection takes place equally in the upper and lower thick layers, and this provides good heat transport [Fig. 9(c)]. However, when more internal sheets are present [Figs. 9(e), (g), (i)], the upper and lower convecting layers are considerably less active, and heat transport is decreased. Results from Fig. 7(c) show that for a constant-pressure upper boundary, σ is reduced for any number of internal sheets. This is explained by observation of Figs. 10(c), (e), (g), (i) where the bottom convecting layer in each case is much less active than those above.

For insulation purposes then, any number of internal sheets inserted into a medium with an open top will improve the properties required, while for a closed top material, at least two internal sheets should be introduced.

5. SUMMARY

The effect of introducing equally-spaced thin sheets of an almost impermeable material into an otherwise homogeneous porous medium has been investigated. It has been found that the temperature difference required to destabilize the system is considerably increased by the presence of these sheets. However, thermal interactions through the sheets tend to mitigate this effect somewhat when the thermal conductivities of all layer materials are equal.

Provided the permeability of the sheets is not too small convection begins on a large scale, i.e. the flow takes place through all layers. However the convection becomes localized in the thicker layers when the sheets are almost impermeable, with a corresponding marked decrease in cell-width and, in most cases, a decrease in heat transport for slightly supercritical Rayleigh numbers.

The introduction of less permeable sheets induces an effective anisotropy in the permeability of the system. Comparison with results for a homogeneous anisotropic layer shows that, provided the effective anisotropy parameter ξ is not too large, the homogeneous system can be used to model the layered systems. However when the sheets become too impermeable, and the convection is of local type, the homogeneous anisotropic model breaks down.

In particular, the use of the homogeneous model to analyse convection in snow where thin icy layers are present has been shown to be valid only when an ice sheet is not the topmost layer. A less permeable ice layer on top promotes recirculation of air within the snow:

this recirculation is much weaker in the homogeneous anisotropic model with a constant-pressure upper boundary condition [10].

It has also been shown that homogeneous insulation materials may be made more effective by the insertion of impermeable sheets at equal spacings. The temperature difference required for convection to begin is increased by the introduction of any number of such internal sheets. The subsequent heat transport is decreased in all cases for a system with a constant-pressure boundary. For a system with an impermeable upper boundary, the rate of heat transport will be decreased by the insertion of at least two internal impermeable sheets.

REFERENCES

1. R. McKibbin and P. A. Tyvand, Anisotropic modelling of thermal convection in multilayered porous media, *J. Fluid Mech.* **118**, 315–339 (1982).
2. O. Kvernfold and P. A. Tyvand, Nonlinear thermal convection in anisotropic porous media, *J. Fluid Mech.* **90**, 609–624 (1979).
3. R. McKibbin and M. J. O'Sullivan, Onset of convection in a layered porous medium heated from below, *J. Fluid Mech.* **96**, 375–393 (1980).
4. R. McKibbin and M. J. O'Sullivan, Heat transfer in a layered porous medium heated from below, *J. Fluid Mech.* **111**, 141–173 (1981).
5. E. Palm and M. Tveitereid, On heat and mass flux through dry snow, *J. Geophys. Res.* **84**, 745–749 (1979).
6. E. Palm and K. Vøllan, On thermal convection in a two-layer model composed of a porous layer and a fluid layer, to be published (1983).
7. M. A. Combarous and S. A. Bories, Hydrothermal convection in saturated porous media, *Adv. Hydrosci.* **10**, 231–307 (1975).
8. P. Cheng, Heat transfer in geothermal systems, *Adv. Heat Transfer* **14**, 1–105 (1978).
9. G. Z. Gershuni and E. M. Zhukhovitskii, *Convective Instability of Incompressible Fluids*, Keter, Jerusalem (1976). [Originally in Russian; Nauka, Moscow (1972).]
10. R. McKibbin, P. A. Tyvand and E. Palm, On the recirculation of fluid in a porous layer heated from below, to be published (1983).
11. D. A. Nield, Onset of thermohaline convection in a porous medium, *Water Resources Res.* **4**, 553–560 (1968).
12. P. J. Burns, L. C. Chow and C. L. Tien, Convection in a vertical slot filled with porous insulation, *Int. J. Heat Mass Transfer* **20**, 919–926 (1977).

APPENDIX

GENERAL FORMULATION OF THE PHYSICAL PROBLEM

A saturated permeable layer of thickness d is considered to be composed of N horizontal layers which are separately homogeneous and isotropic (Fig. 15). Layer i has thickness d_i , permeability K_i , and, when saturated, thermal conductivity k_i , each of which may vary from layer to layer. The system is bounded below by an impermeable isothermal surface at temperature $T_s + \Delta T$. Here T_s is the uniform temperature of the top surface, which is considered to be either impermeable ('closed top') or at a constant pressure ('open top').

For small-amplitude convection in the system, only steady solutions are of interest. For such flows which are 2-dim. and confined to the region $\{(x, z): 0 < x < l, 0 < z < d\}$, the usual

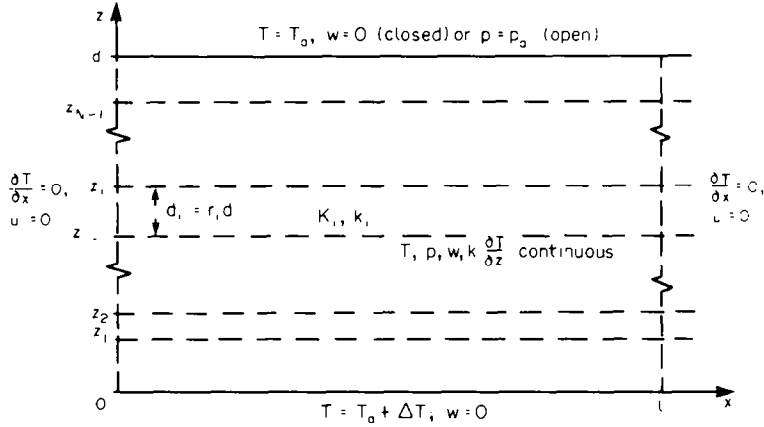


FIG. 15. Schematic diagram of the configuration considered—a porous medium composed of N homogeneous horizontal layers.

equations of conservation of mass and energy and Darcy's law become, within layer i ,

$$\frac{\partial u}{\partial x} + \frac{\partial w}{\partial z} = 0, \quad (\text{A1})$$

$$c \left(u \frac{\partial T}{\partial x} + w \frac{\partial T}{\partial z} \right) = k_i \left(\frac{\partial^2 T}{\partial x^2} + \frac{\partial^2 T}{\partial z^2} \right), \quad (\text{A2})$$

$$\frac{\partial p}{\partial x} = - \frac{\nu}{K_i} u, \quad (\text{A3})$$

$$\frac{\partial p}{\partial z} = - \rho_s [1 - \alpha(T - T_0)] g - \frac{\nu}{K_i} w. \quad (\text{A4})$$

Here (u, w) is the mass flux vector of the fluid, which has kinematic viscosity ν and specific heat c , both assumed constants, and density $\rho = \rho_s [1 - \alpha(T - T_0)]$, where ρ_s is the density at temperature T_0 and α is the coefficient of thermal expansion. T and p are the temperature and pressure at a point within the saturated medium.

The boundary conditions at the bottom and the top of the system are

$$T = T_0 + \Delta T \text{ and } w = 0 \text{ on } z = 0,$$

$$T = T_0 \text{ and } \begin{cases} w = 0 \text{ (closed top)} \\ p = p_0 \text{ (open top)} \end{cases} \text{ on } z = d.$$

At each interface, continuity of temperature, pressure, vertical mass flux and vertical heat flux requires that T , p , w and $cT w - k(\partial T / \partial z)$ be continuous. On the vertical lateral boundaries at $x = 0$ and l , which may be physical sidewalls (assumed insulated) or cell-cell interfaces in a spatially-periodic convection pattern confined between such sidewalls, the boundary conditions are that no horizontal heat or mass flow takes place, and therefore

$$\frac{\partial T}{\partial x} = 0 \text{ and } u = 0 \text{ on } x = 0, l.$$

The flow of heat through the system may be measured by the mean vertical heat flux Q , which, evaluated at the base of the system, is given by

$$Q = \frac{1}{l} \int_0^l -k_1 \left(\frac{\partial T}{\partial z} \right)_{z=0} dx. \quad (\text{A5})$$

The basic procedure, to determine the solution to equations (A1)–(A4) subject to the boundary conditions and hence to evaluate Q , is to investigate small perturbations to the conduction solution ($u = w = 0$). The conduction solution for

the temperature, T_c , is a piecewise linear function given by

$$T_c = T_0 + \Delta T \left(\sum_{j=i}^N \frac{d_j}{k_j} - \frac{z - z_{i-1}}{k_i} \right) / \sum_{j=1}^N \frac{d_j}{k_j} \quad (\text{A6})$$

for $z_{i-1} < z < z_i$, where $z_i = \sum_{j=1}^i d_j$, $i = 1, 2, \dots, N$. The pressure distribution p_c for the conduction solution is obtained from T_c by using equation (A4) and the requirement that p_c be continuous at each interface. The heat flux Q_c corresponding to this conduction solution is, from equations (A5) and (A6),

$$Q_c = \Delta T / \sum_{j=1}^N \frac{d_j}{k_j}. \quad (\text{A7})$$

Variations from the conduction solution are studied by substituting $u = u'$, $w = w'$, $T = T_c + T'$ and $p = p_c + p'$ in equations (A1)–(A4) and the boundary conditions. Writing u' and w' in terms of a stream function ψ , and eliminating p' , results in a set of partial differential equations in T' and ψ with a set of $4N$ boundary conditions for those quantities.

For a given physical configuration, there is a smallest value of ΔT , denoted ΔT_c , which can produce the onset of convection. This corresponds to the critical value R_c of the Rayleigh number R for the system, defined by

$$R = \frac{\rho_s g c \alpha K_1 \Delta T d}{4 \pi^2 \nu k_1}. \quad (\text{A8})$$

For values of ΔT above ΔT_c ($R > R_c$), a finite-amplitude flow can exist. A perturbation parameter ζ is defined by

$$\zeta^2 = (\Delta T - \Delta T_c) / \Delta T = (R - R_c) / R.$$

Then T' , ψ and R are expanded as power series in ζ

$$T' = \zeta T^{(1)} + \zeta^2 T^{(2)} + \dots,$$

$$\psi = \zeta \psi^{(1)} + \zeta^2 \psi^{(2)} + \dots,$$

$$R = R_c + R_c^{(1)} \zeta^2 + R_c^{(2)} \zeta^4 + \dots + R_c^{(2s)} \zeta^{2s}$$

where $R_c^{(s)} = R_c / (1 - \zeta^{2s})$. These series are substituted in equations (A1)–(A4) and the boundary conditions, and give rise to a sequence of problems, each associated with a different power of ζ [3, 4].

The solution of the $O(\zeta)$ problem allows calculation of R_c and the shape of the streamlines and isotherms (equal temperature departures from the conduction solution) at onset of convection. The value of R_c depends on the layered configuration and also on the non-dimensional cell-width $L = l/d$. Subsequent solution of the $O(\zeta^2)$ and $O(\zeta^3)$ problems allows calculation of the non-dimensional vertical heat

flux to $O(\zeta^2)$. This is expressed by the Nusselt number Nu , where $Nu = Q/Q_c$, in the form

$$Nu = 1 + \sigma \left(\frac{R}{R_c} - 1 \right); \quad R > R_c \quad (A9)$$

where σ is a constant which depends on the system configuration, the cell-width L and the upper boundary condition. For $R \leq R_c$, $Nu = 1$.

The value of R_c for a given system depends on L ; the minimum value is denoted by $R_{c\min}$, given at $L = L_c$. These values correspond to the preferred onset mode in a system of infinite width. For a homogeneous isotropic layer with a closed top, $R_{c\min} = 1.0$ and $L_c = 1.0$, with a corresponding value of $\sigma = 2.0$. For an open top, the values are $R_{c\min} = 0.686$, $L_c = 1.35$ and $\sigma = 1.95$.

For the systems considered in this paper, it is assumed that alternate layers have the same material properties and thickness. The systems can therefore be characterized by layers 1 and 2; for $N > 2$, this pair of layers is repeated in the configuration. Thus $d_1 + d_2 = 2d/N$. Writing $d_2/(d_1 + d_2) = \varepsilon$, $K_2/K_1 = \beta$ and $k_2/k_1 = \gamma$, estimates of induced anisotropy in permeability and conductivity in the system are found to be,

respectively,

$$\begin{aligned} \xi &= \frac{K_H}{K_V} = [1 - \varepsilon + \varepsilon\beta] \left[\frac{1 - \varepsilon + \frac{\varepsilon}{\beta}}{\beta} \right], \\ \eta &= \frac{k_H}{k_V} = [1 - \varepsilon + \varepsilon\gamma] \left[\frac{1 - \varepsilon + \frac{\varepsilon}{\gamma}}{\gamma} \right]. \end{aligned} \quad (A10)$$

Here K_H , K_V and k_H , k_V are average permeabilities and conductivities in the horizontal (subscript H) and vertical (subscript V) directions (see ref. [1], Section 2).

A Rayleigh number R^* may be defined in terms of K_V and k_V by

$$R^* = \frac{\rho_a g \alpha K_V \Delta T d}{4\pi^2 \nu k_V} \quad (A11)$$

From equation (A8), R^* is proportional to R , and also takes its minimum value $R_{c\min}^*$ at $L = L_c$, where

$$R_{c\min}^* = \left[\frac{1 - \varepsilon + (\varepsilon/\gamma)}{1 - \varepsilon + (\varepsilon/\beta)} \right] R_{c\min} \quad (A12)$$

Values of $R_{c\min}^*$, L_c and corresponding σ for a homogeneous anisotropic layer with either a closed top or an open top were given in ref. [1].

CONVECTION THERMIQUE DANS UN MILIEU POREUX COMPOSE DE COUCHES ALTERNATIVEMENT EPAISSES ET MINCES

Résumé - Cet article est la suite d'un récent travail des auteurs [*J. Fluid Mech.* **118**, 315-339 (1982)]. Le texte précédent se concentre sur la convection naturelle dans un milieu poreux composé de couches alternées d'épaisseur égale. Ici on étudie le cas limite où chaque couche est très mince et a une perméabilité très faible. L'établissement de la convection dans un tel système et le flux thermique à des nombres de Rayleigh légèrement supercritiques sont étudiés. Comme dans le travail précédent, on fait une étude de la convergence à l'anisotropie homogène: un développement est réservé à l'application aux techniques d'isolation et à la convection dans les couches de neige.

FREIE KONVEKTION IN EINEM PORÖSEN MEDIUM, DAS AUS ABWECHSELND DICKEN UND DÜNNEN SCHICHTEN BESTEHT

Zusammenfassung - Die Arbeit ist die Fortsetzung einer vorausgegangenen Veröffentlichung der gleichen Autoren. Die vorhergehende Arbeit bezog sich auf die freie Konvektion in einem porösen Medium, das aus Schichten abwechselnden Materials von gleicher Dicke bestand. Diese Arbeit ist eine Studie für den Grenzfall, bei dem jede zweite Schicht sehr dünn ist und eine sehr geringe Durchlässigkeit hat. Es wird das Einsetzen der Konvektion in einem solchen System und der Wärmestrom bei leicht überkritischen Rayleigh-Zahlen untersucht. Wie in der früheren Arbeit wird auch hier eine Untersuchung der Konvergenz in Richtung homogener Anisotropie durchgeführt. Hingewiesen wird auf Anwendungen in der Isoliertechnik und auf das Problem der Konvektion in Schneeschichten.

ТЕПЛОВАЯ КОНВЕКЦИЯ В ПОРИСТОЙ СРЕДЕ, СОСТАВЛЕННОЙ ИЗ ЧЕРЕДУЮЩИХСЯ СЛОЕВ БОЛЬШОЙ И МАЛОЙ ТОЛЩИНЫ

Аннотация Данное исследование является продолжением предыдущей работы авторов, опубликованной в Журнале по механике жидкостей (*J. Fluid Mech.*) т. **118**, стр. 315-339, 1982 г., в которой исследовалась свободная конвекция в пористой среде, составленной из слоев одинаковой толщины. В настоящей работе исследуется предельный случай, когда каждый второй слой имеет очень малую толщину и проницаемость. Рассматривается возникновение конвекции в такой системе и определяется величина теплового потока при небольшом превышении критического числа Рэлея. Как и в предыдущей работе, исследуется переход к однородной анизотропии. Кроме того, особое внимание обращено на прикладные аспекты исследования (теплоизоляция и конвекция в снежном покрове).